U.S. Naval Air Development Center

Johnsville, Pennsylvania
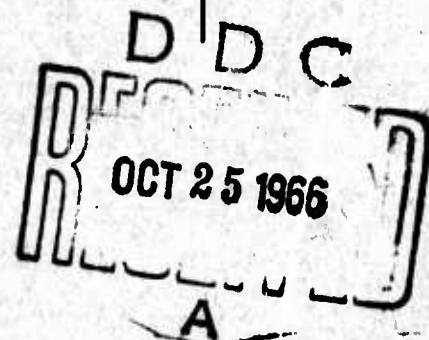
REPORT NO. NADC-AE-6620   6 SEP 1966

DYNAMIC CHARACTERISTICS OF UNDERWATER CABLES
FLOW INDUCED TRANSVERSE VIBRATIONS

WEPTASK NO. ASW213000/2011/W210-14-00
Problem No. 803

Distribution of this document is unlimited.

Limitations concerning the distribution of
this report and revelation of its contents
appear on the inside of this cover.

DEPARTMENT OF THE NAVY
U. S. NAVAL AIR DEVELOPMENT CENTER
JOHNSVILLE·
WARMINSTER, PA. 18974

Aero-Electronic Technology Department

REPORT NO. NADC-AE-6620   6 September 1966

DYNAMIC CHARACTERISTICS OF UNDERWATER CABLES
FLOW INDUCED TRANSVERSE VIBRATIONS

WEPTASK NO. ASW213000/2011/W210-14-00
Problem No. 803

The dynamic behavior of strumming hydrophone cables associated
with air-launched sonobuoy surveillance systems is reported for
a 200 to 3000 Reynolds number range. The study techniques and
the scaling laws have application wherever underwater flexible
cables are employed. Results are reported in four specific
areas: experimental diagnostic techniques, cable tuning effects,
frequency scaling law, and dynamic motion analysis.

Submitted by: J. Dale   H. Menzel   J. McCandless
                 Sonar Sensor Division

Approved by: H. Suter, Superintendent
                 Sonar Sensor Division

                 Donald Mackiernan
                 Technical Director

Distribution of this document is unlimited.

S U M M A R Y

INTRODUCTION

The dynamic behavior of strumming hydrophone cables associated with
air-launched sonobuoy surveillance systems is reported for a 200 to 3000
Reynolds number range. The study techniques employed and the scaling laws
formulated have application wherever underwater flexible cables are
employed.

RESULTS

Results are reported in four specific areas:

1. Experimental Diagnostic Techniques - Techniques are developed for
analyzing the vibrational characteristics of a smooth flexible cable
supporting a spherical terminal mass (hydrophone).

2. Cable Tuning Effects - Tuning characteristics are experimentally and
analytically analyzed for various cable parameters.

3. Frequency Scaling Law - The classical Strouhal number concept is
modified to include the effects of flow at any angle incidence to the
cable and a larger virtual cable diameter resulting from cable vibration
transverse to the flow field.

4. Dynamic Motion Analysis - A tractable analytical model is developed
which defines the motion of the terminal mass, forced by the transverse
cable vibration.

CONCLUSIONS

1. Flexible cable tuning phenomenon has been observed and analyzed for
a strumming cable supporting a terminal weight in a varying velocity
water flow field. Discrete vibration mode transitions have been inter-
preted as defining frequency intervals which characterize the fundamen-
tal or partial standing wave vibration modes. Analytical correlation
with these tuning effects has been obtained using the classical vibrating
string relation.

$$n = 2 \, f_V \, L \, \sqrt{\frac{w_c}{T}}$$

where a virtual specific mass involving the specific cable mass plus the
mass of an equivalent volume of water is used for w_c.

Long cable tuning effects are characterized by random periods of atten-
uated cable vibrations usually accompanied by multiple frequency beat

effects. The SHORT cable tuning effects show negligible cable vibration at water velocities less than the minimum velocity which excites the fundamental standing wave.

2. A modified version of the classical Strouhal number has been empirically determined. This version corrects for the flow incidence angle of a streaming cable and assumes a larger virtual diameter for the strumming cable. The relation has the form

$$f_v = k \frac{u_o \sin \theta}{d(u_o \sin \theta)^m},$$

and it correlates with experimental data to within 5 percent.

3. The analytical motion analysis shows reasonable correlation with experimental data considering the linearizing assumptions used. Vertical resonance of the submerged cable and terminal mass is shown to shift to the longer standing wave lengths for longer submerged cable lengths. When the water velocity corresponds to a forcing frequency that is equivalent to a true partial vibration frequency concomitant with the vertical resonance frequency, large amplitude vibrations of the terminal mass result. When a motion sensitive hydrophone is the terminal mass, extreme pseudo-acoustic signals result.

4. Cable strumming diagnostics are enhanced by interpreting the ensuing signals from a hydrophone used as a terminal mass.

NADC-AE-6620

T A B L E   O F   C O N T E N T S

LIST OF FIGURES

L I S T   O F   S Y M B O L S

a, b, c - Constants, see text

C_L - Lift coefficient

d   - Flexible cable diameter

D   - Diameter of spherical terminal mass

e   - Constant, see text

f   - Frequency of periodic function

F   - Periodic force

g   - Gravitational constant

h   - Constant, see text

k   - Constant, see text

K   - Spring constant per foot of cable

K_x - Equivalent spring constant per standing wave, transverse to the cable

ℓ - Length of one standing wave

L   - Total submerged cable length

$\Delta\ell$ - Change in cable length over one standing wave

m   - Constant, see text

mv   - Peak-to-peak hydrophone signal amplitude in millivolts

n   - Number of standing waves over length (L)

N_{Re} - Dimensionless Reynold's number, du/μ

r   - Fluid damping constant

S_t - Dimensionless Strouhal number, df/u

t   - Time

T   - Tension in the flexible cable

u   - Water velocity

w   - Virtual specific mass of the cable (mass per unit length). Equals the sum of the specific cable mass and an equivalent mass of water

W   - Virtual mass of the terminal hydrophone

x   - Displacement of the transverse cable vibrations

y   - Displacement of the terminal mass parallel to the cable

LIST OF SYMBOLS (continued)

α - Phase angle between vertical force and acceleration

β - Constant defined by analysis

δ - Vertical static spring deflection

ϕ - Phase angle between vertical force and displacement

θ - Flow incidence angle, acute angle between horizontal flow field and the cable tangent

ρ - Water mass density

μ - Water viscosity

ω - Angular frequency of a periodic function

Δ - Incremental change

γ - Phase angle between horizontal force and displacement

τ - Period of periodic motion

LIST OF SUBSCRIPTS

c   - Flexible cable parameter

f   - Refers to the alternate periodic shedding fluid vorticies

m   - Terminal mass parameter

o   - Free stream water parameter

s   - Refers to a characteristic of the hydrophone signal

v   - Vibrating cable parameter

y   - Refers to a direction parallel to the flexible cable

D I S C U S S I O N

BACKGROUND

Moored or drifting sonar surveillance systems suspend a sonar transducer by means of an underwater cable. The transducers are usually single element or line array hydrophones attached to supporting cables in complex arrangements of short cables and line mass. The transducers are frequently suspended at depths where horizontal shear currents interact with the flexible cables causing periodic cable vibrations, commonly called cable strumming. This periodic strumming causes pseudo-acoustic signals from the hydrophones, and it interferes with the surveillance function.

A cursory study[1] revealed the presence of discrete standing wave cable vibrations with the same period as the shedding fluid vortices. The non-dimensional Strouhal number (S_t) and the classical string equation,

$$\ell = \frac{1}{2f} \sqrt{\frac{T}{w}} \tag{1}$$

were approximately correlated with the experimental data. Experimental frequency data was obtained by means of a tensiometer supporting a free streaming cable. Data was taken at discrete velocities between 0.6 and 1.5 knots and analyzed to determine prominent frequency spectra. Prominent frequencies were obtained which correlated with the alternately shedding vortices, commonly associated with the side lift forces, and the oscillating drag forces. Also, evidence was found for the vibration frequency to be dependent on the streaming angle of the cable as well as the free stream velocity and cable diameter.

The dynamic cable characteristics reported here are the results of a study of the flow-induced transverse vibrations of a variable length 0.1-inch diameter smooth cable in the 200 to 3000 Reynolds number range (0.25 to 1.5 knots water velocity range).

---

1. Dale, J. R., and Menzel, H. R., Dec 1965; Flow Induced Oscillations of Hydrophone Cables; NAVAIRDEVCEN; 23 rd Naval Underwater Sound Symposium Proceedings.

The following technical interpretations are to be construed throughout this report:

1. For a finite length (L) of submerged cable, the vibrations discussed are related to standing wave vibrations associated with the fundamental or specific partial frequencies. A partial frequency is higher than the fundamental, but not a true harmonic, because the frequency is not an exact multiple of the fundamental. The fluid lift forces acting at the sides of the cable comprise the periodic forcing function for all the standing-wave vibrations discussed. The rear acting periodic drag forces, known to be twice this frequency, are not considered.

2. When the standing waves vibrate at a frequency corresponding to the true fundamental or true partial frequency, such correspondence is termed horizontal resonance. Vertical resonance is mechanical resonance of the cable (spring) and terminal weight (mass) of the cable.

3. Unless stated otherwise, the physical test model consists of a variable length 0.107-inch diameter smooth coaxial cable rigidly fixed at the upper end and supporting a 2-inch diameter 0.8 pound spherical terminal weight (piezoelectric type hydrophone - approximate acoustic sensitivity is -84 dbv/ub). This model was chosen because of its basic geometry, thus affording some simplification of the dynamic motion analysis.

Vibration diagnostics were enhanced by using a typical hydrophone as the terminal mass and interpreting the associated electrical signals in terms of the cable vibrational characteristics. The signals are predominantly accelerations of the hydrophone parallel to the attached cable. Steady state cable strumming can physically be interpreted as a continuous series of standing waves along the length of the cable that periodically vary the cable tension. This results in a low amplitude periodic hydrophone motion in line with the supporting cable. Some inherent second order hydrophone effects that contribute to the signal are water loading, static head variations, and rocking motions. When such a system is used as an underwater acoustic sensor, these pseudo-acoustic effects are summed as the integrated signal.

The manifold wave form characteristics of the hydrophone signals were easily identified by the repeating bizarre wave forms. Typical characteristics are categorized in figure 1. Note - the signal frequency is twice the cable vibration or alternate shedding vortex frequency. This occurs because the mass is accelerated upward each time the cable motion is away from its centerline position. The periodic signals have a very irregular appearance above a Reynolds number of 1000, making diagnostics
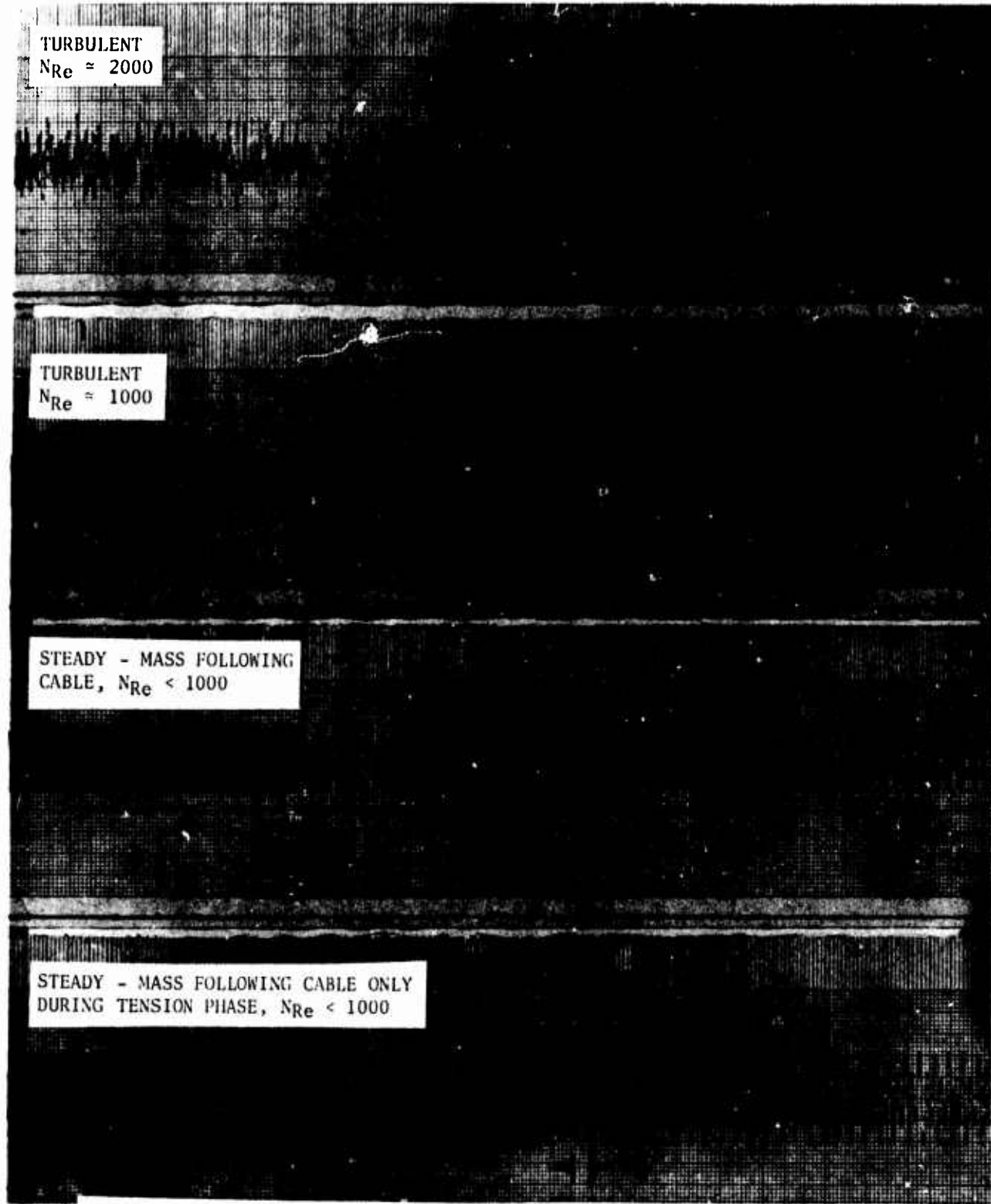
NOTE: PERIOD OF CABLE VIBRATION IS INDICATED. 1 SECOND TIME PULSES ARE
INDICATED BELOW EACH RECORD. PAPER SPEED CHANGED FROM 20 TO 100 MM/SEC.

FIGURE 1 - Hydrophone Signal Wave Forms

difficult. Wave cavitation near the water surface was observed, and it
is assumed that it distorts the signal structure above this Reynolds
number. When the mass follows the vertical perturbations of the cable
during both the tension and relaxation strokes of the cable, the wave
form is near sinusoidal - otherwise the mass tends to float downward dur-
ing the relaxation stroke and distorts that portion of the wave form.

Another diagnostic stratagem which proved extremely valuable was to
slowly vary the water flow field from about 1.2 to 0.25 knots and inter-
pret the resulting signal signature in terms of a cable tuning effect.
(Note - the term "signal signature" is used with reference to the overall
characteristic for a given water velocity range.) This effect refers to
discrete cable vibration modes that ensue when the cable vibrates through
a frequency range representing more than one numbered partial. To obtain
this flow variation, a long weighted chain drove a radial cable support
arm by means of ropes and pulleys. The chain gradually unloaded the drive
force as it piled on the floor. This device proved to be acoustically
quiet with negligible mechanical vibration.

STANDING WAVE TRANSITIONS

Typical signal signatures are shown in figure 2 for submerged cable
lengths (L) of 3, 6, and 12 feet when the flow field decreased from
about 1.2 to 0.2 knots. The aesthetic overall characteristic and the
sharp amplitude transitions at discrete velocity increments should be
noted. The transitions occur more frequently as L increases; however,
they are better defined for the short lengths where the streaming cable
geometry has a smaller angle variation.

When the vibration frequency (f_v) is plotted against free stream
velocity (u_0), as in figures 3 and 4, the transitions are seen also to
be characterized by discrete frequency transitions. (Note - the frequency
transitions occur at the same velocity as the amplitude transitions which
are reproduced as the lower curve.) A mean curve drawn through the plot
shows the frequency to be above the line immediately after the transition
for increasing velocity and below the line prior to the next transition.

An expanded section of the record, at transition, recorded at a paper
speed of 100 mm/second is shown in figure 5. A marked change can be seen
in the regularity of the waveform indicating a change in the vibrational
mode of the terminal mass. Also, at transition the vertical motion
appears to go out of syncronization with the periodic cable forces, thus
reducing the amplitude to practically zero. This occurs over a velocity
change of the order of 0.01 knots. A typical signal structure between
transitions also is shown in figure 5 where a clearly defined maximum
level is seen. (Note - the term "signal structure" is used with reference
to a localized characteristic of the signal signature.)

3 FOOT CABLE

6 FOOT CABLE

12 FOOT CABLE

NOTE: THE SHARP AMPLITUDE TRANSITIONS CHARACTERIZE A CHANGE IN THE NUMBER OF STANDING WAVES. WATER VELOCITY DECREASES TO THE RIGHT FROM 1.2 KNOTS TO 0.2 KNOTS. 1 SECOND TIME PULSES ARE INDICATED BELOW EACH RECORD.

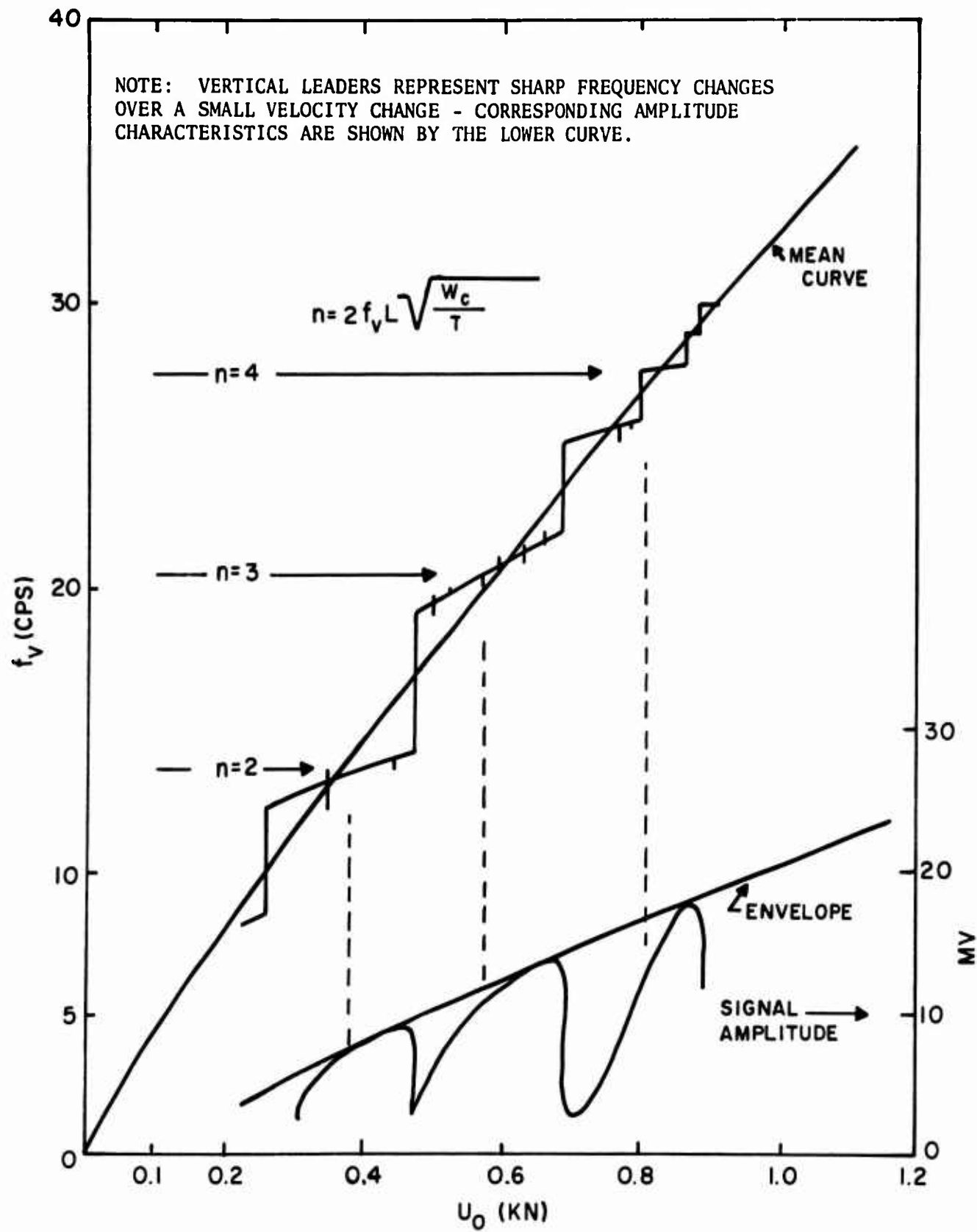FIGURE 2 - Signal Structures from the Terminal Hydrophone

FIGURE 3 - Frequency Characteristics for 3-ft long
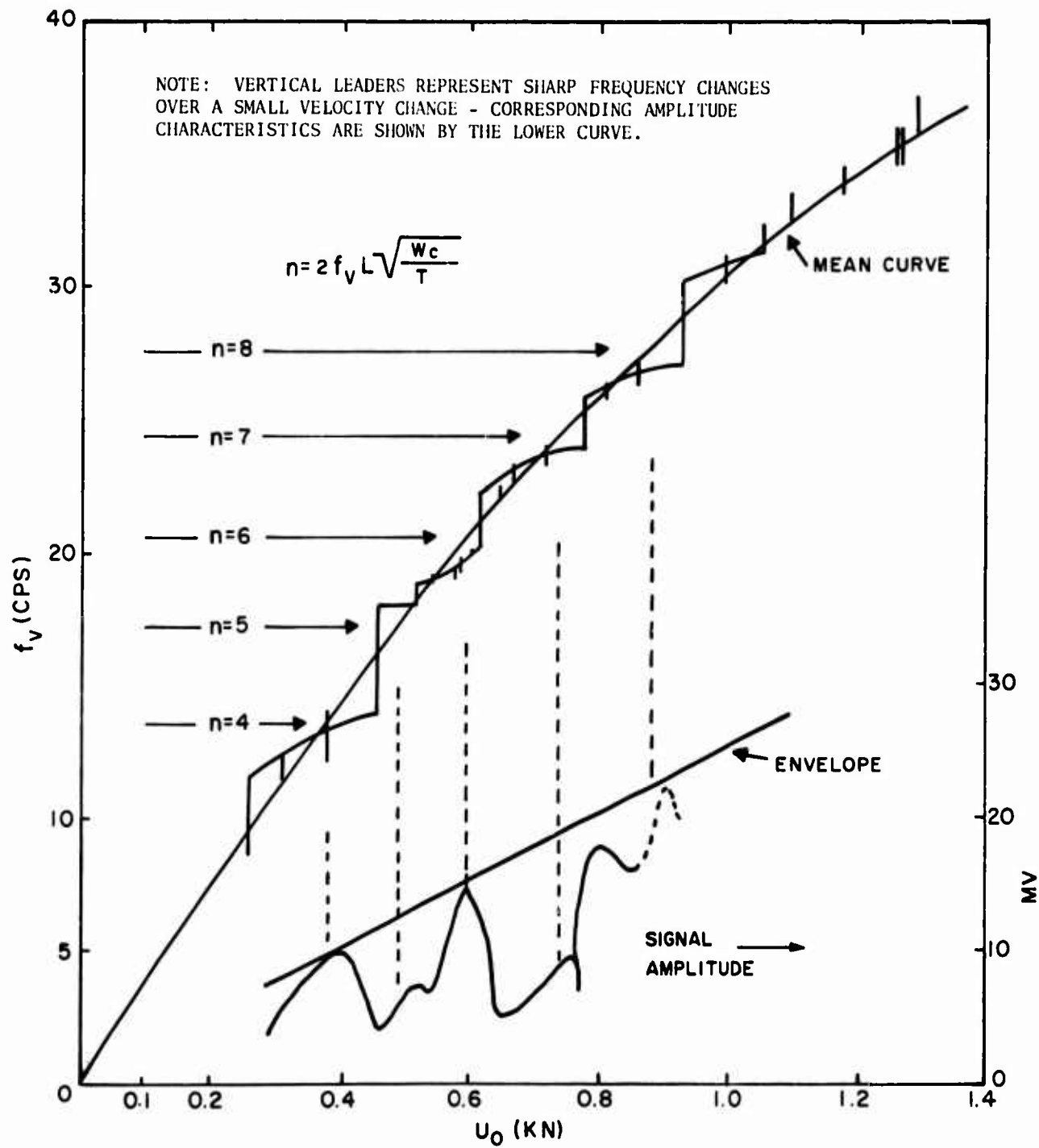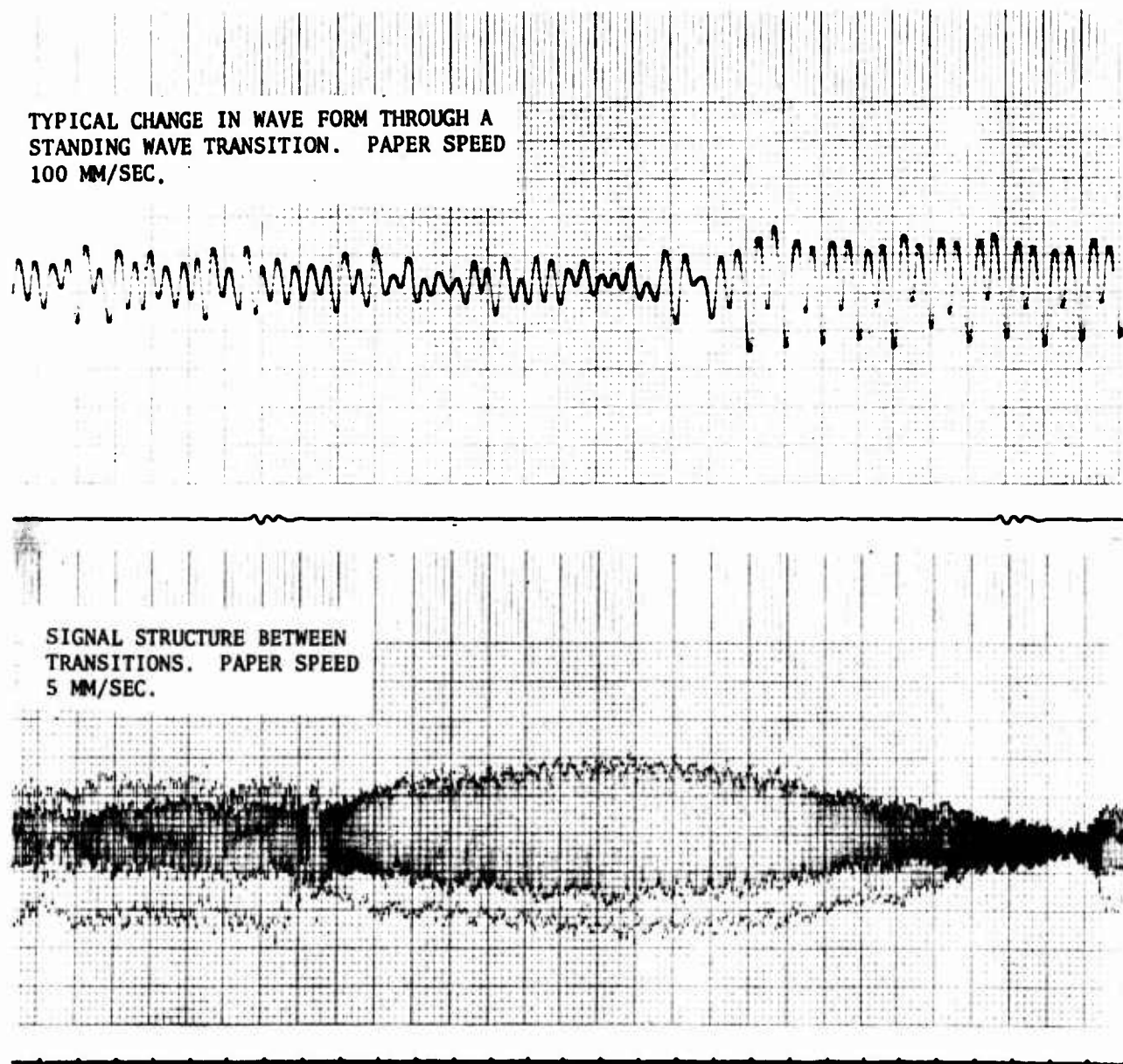0.1-in. Diameter Flexible Cable

FIGURE 4 - Frequency Characteristics for 6-ft long
0.1-in. Diameter Flexible Cable

TYPICAL CHANGE IN WAVE FORM THROUGH A
STANDING WAVE TRANSITION. PAPER SPEED
100 MM/SEC.

SIGNAL STRUCTURE BETWEEN
TRANSITIONS. PAPER SPEED
5 MM/SEC.

NOTE: WATER VELOCITY DECREASES TO THE RIGHT. 1 SECOND TIME PULSES ARE
INDICATED BELOW EACH RECORD.

FIGURE 5 - Characteristics of Partial Vibrations

The physical concept developed from this data ascribes that the signal structure between adjacent transitions defines a discrete partial vibration frequency interval. The transitional limits of this interval are analogous to musical sharps or flats because they represent vibrations that are approximately one-half partial higher or lower than the true partial frequency. As the free stream velocity increases, representing the forcing frequency, a critical (transitional) cable vibration frequency is reached where it is unstable by virtue of a marked amplitude attenuation. This attenuation results from the inability of the cable to follow the periodic fluid forces that try to force the cable at a frequency higher than the damped natural cable frequency for that particular partial number of waves. During this incipient state, the quasi-stationary cable is sympathetic to the fluid forcing frequency which is characterized by the higher frequency point on the mean curve (figure 3) for the same water velocity. The next higher numbered partial vibration is more stable at this higher frequency because its damped natural frequency is higher than the forcing frequency, and the cable can respond with higher fidelity. The actual frequency transition extends past the mean curve frequency and approaches the true partial frequency. The steady vibrations now start to increase in amplitude with increasing frequency because the fluid forces increase with velocity and the true partial vibration (horizontal resonance) is approached - thus, the triangular appearance. The high amplitude cable vibrations must have a strong stabilizing effect on the spanwise in-phase relationship of the fluid forces, so that the fluid forces are in phase over the complete standing wave length (ℓ). The transverse cable displacement would be 180 degrees out of phase for adjacent standing waves. Through transition, the sympathetic cable vibrations must force a spanwise in-phase correlation for the new standing wave length.

As the water velocity continues to increase, the forcing frequency reaches the damped natural cable frequency and the true partial vibration (horizontal resonance) results. Resonance is assumed to occur between transitions approximately where the mean frequency curve (figure 3) intercepts the actual curve. As the water velocity increases from the true partial point to the transition point, the vibration amplitude is progressively attenuated due to the higher forcing frequency which continues to increase above the damped natural system frequency. With increasing water velocity, the transition, amplification, and attenuation phases continue to repeat.

The similarity between these results and the results of both Windhorst[2] and Warren[3] are interesting. Instead of a flexible cable, these investigators used oscillating rigid cylinders in water flow fields. Windhorst reports an increase in cylinder amplitude and frequency when the

2. *Meier-Windhorst, August, 1939; Flow Induced Vibrations of Cylinders in Uniform Flow, Munich Technische Hochschule, Hydraulische Inst. Mitt., Heft 9.*

3. *Warren, Dr. W. F., 1962; An Experimental Investigation of Fluid Forces on an Oscillating Cylinder; University of Maryland.*

water velocity was increased to a critical value, where the water forced vibrations occur at the damped natural system frequency. Then in the supercritical range, the amplitude drops sharply and the frequency raises similar to the transitional effects reported in this present study. A close look at the frequency characteristics between transition on figures 3 and 4 does show some secondary transitions near the proposed true partial frequencies accompanied by a high amplitude signal. Both the primary and secondary transitional effects correlate well with Windhorst's work.

Warren reports an increase in the lift force when the water velocity is increased to a value where the free vortices form at the same frequency as the forced oscillation. The force drops sharply at water velocities above or below this value. Since the amplitude of a free cylinder would be expected to follow the lift force effect, this data is seen to correlate with the previous data.

With regard to the slope of the frequency curves (figures 3 and 4) between primary transitions, Windhorst states that as the cable vibration amplitude increases the water is exchanging energy to the cable, and the frequency approaches that value defined by the Strouhal concept (approximately by the mean curve of figures 3 and 4). As the cable vibration amplitude decreases the energy exchange is from the cable to the water, and at times no free vortices are observed. The vibration frequency diverges from that defined by the Strouhal concept. These conclusions apparently apply as well to a flexible cable because the frequency curve between transitions crosses the mean curve at a velocity approximating the peak signal amplitude.

The transitions then characterize one more or one less standing wave depending on whether the water velocity is increasing or decreasing; also, between any two adjacent transitions there occurs a horizontal resonant condition representing the true partial vibration.

To further validate this concept, the simple undamaged string equation was thought to apply with sufficient accuracy because the fluid damping effect on the vibrating cable is reputed to be small. This equation implies that the partial frequencies are true multiples of the fundamental and are literally harmonics; however, since only low numbered partials are considered, the frequency error is probably small. This equation then provides a means of approximating the true partial frequency for each standing wave. By substituting $\ell = L/n$ in the string equation (1) and using the virtual specific cable mass for w_c, the following relation for n is obtained:

$$n = 2 f_v L \sqrt{\frac{w_c}{T}} \tag{2}$$

where the virtual specific mass w_c is the sum of the specific mass of the cable plus the mass of an equivalent volume of water. The virtual mass concept has been substantiated by Windhorst[2] and Warren[3].

The computed values of f_v for the true n partials at submerged lengths of 3 and 6 feet are indicated on the frequency-velocity plots, figures 3 and 4, respectively. The signal amplitude in millivolts is also plotted for correlation. The true n partial vibrations appear to correlate well with the free stream velocity that is between two adjacent transitions, and the projections tend to line up with the velocities equivalent to peak signal levels per partial vibration. This close correlation appears to indicate that the true partial or horizontal resonant vibration occurs at a discrete velocity between transitions. For some partials the transitional velocities appear to be asymmetrical with the resonant velocities, which is indicative of nonrepeatability or a hysteresis effect in the absolute value of the transitional velocity. This has been substantiated by comparing identical transitions from repeated tests. Intuitively, one might suppose that once the fluid vortices lock-on or are forced into a spanwise in-phase relation over each standing wave length, they become stabilized by the cable vibrations and are reluctant to adjust to the new ℓ characterized by the next partial vibration.

The signal signature for the 12-foot length of cable is not characterized by the discrete triangles indicative of each partial vibration interval. This is evident from figure 2 (L = 12 ft), particularly at the higher water velocities. Because the longer cable with the terminal mass streams through a wider range of flow incidence angles, the complex cable vibration modes must interact to form the irregular signature. This effect has been named the "long" cable effect in contrast to the shorter cable lengths where each partial vibration interval is defined.

An oversimplified model of the long cable would assume the cable to be represented by two straight line segments, each having a different flow incidence angle. Then, each segment would be the source of traveling waves generated at a frequency dependent on the flow incidence angle. The hydrophone would be excited by the mean of the two frequencies and the interaction would result in a low-beat frequency or the difference between the two frequencies. Bent frequencies of the order of 2 to 4 cps are estimated considering the variation in flow incidence angle for the 12-foot length at about 1 knot water velocity. The mean frequency signal on the left side of figure 3 (L = 12 feet) is seen to be modulated by beats of this order of frequency. This beat effect appears to attenuate the signal amplitude and probably the cable vibration amplitude.

---

2. *See pg 8.*

3. *See pg 8.*

Another cause of irregularity of the signal structure at the higher water velocities is the complex transitional interactions resulting from the multiple frequencies. Also, typical variations of 10 percent in the static cable tension through transition have been measured. This would cause a sudden change in the standing wave length, and the associated transitions would appear more irregular.

When the cable length is decreased or the cable diameter is increased so that the highest velocity or forcing frequency corresponds to the fundamental standing wave, negligible vibrations occur at lower water velocities. This "short" cable effect may prove useful for inhibiting cable vibrations. The short cable can also be simulated by forcing a nodal point on the cable by addition of mass or a flow-splitter tab at the antinode of the fundamental.

CORRELATION OF FLUID FORCING FREQUENCY

The classical dimensionless Strouhal number relates the alternate vortex shedding frequency characteristic of the flow past a blunt body to the fluid velocity normal to the axis of the body and an appropriate body diameter.

$$S_t = fd/u \qquad (3)$$

This concept must be revised for a flexible strumming cable that is streaming in a static balance between fluid and gravity forces. First, the cable has a virtual diameter which is larger than the actual diameter because of the high frequency vibrations with amplitude of 1 to 3 diameters. Secondly, since it would be desirable to use the free stream velocity for the frequency calculation, a cable angle correction for the streaming cable seems appropriate.

A relationship has been developed which shows reasonable correlation over a limited range of flow incidence angles and cable diameters. The frequency-velocity plot of figure 6 shows the mean curves for submerged lengths of 3, 6, and 12 feet for the 0.107 inch cable diameter and a 6-foot length curve of a 0.25 inch diameter. When the flow incidence angle for the 0.107 inch diameter cable, at the fixed cable end or water surface, was used to correct for the free stream velocity component normal to this end of the cable, all curves coincided within 5 percent with the 3-foot curve (common correlation curve). Incidence angles for the 3-foot cable resulted in a negligible correction. The 0.25 inch diameter curve also showed common correlation considering the angle correction and the inverse diameter relation. As a further check on this correlation curve, 6-foot lengths of 0.075, 0.107, and 0.150 inch diameter cables were supported at both ends to negate the angle effect. Correlation was again obtained with the common curve.

$$f = \frac{0.29\, U_0 \sin\theta}{d(U_0 \sin\theta)^{0.12}}$$

L= 3'

COMMON CORRELATION CURVE

L= 6'

L=12'

*d = 0.107"

L= 6'

d= 0.25"

f_v (CPS)

40

30

20

10

5

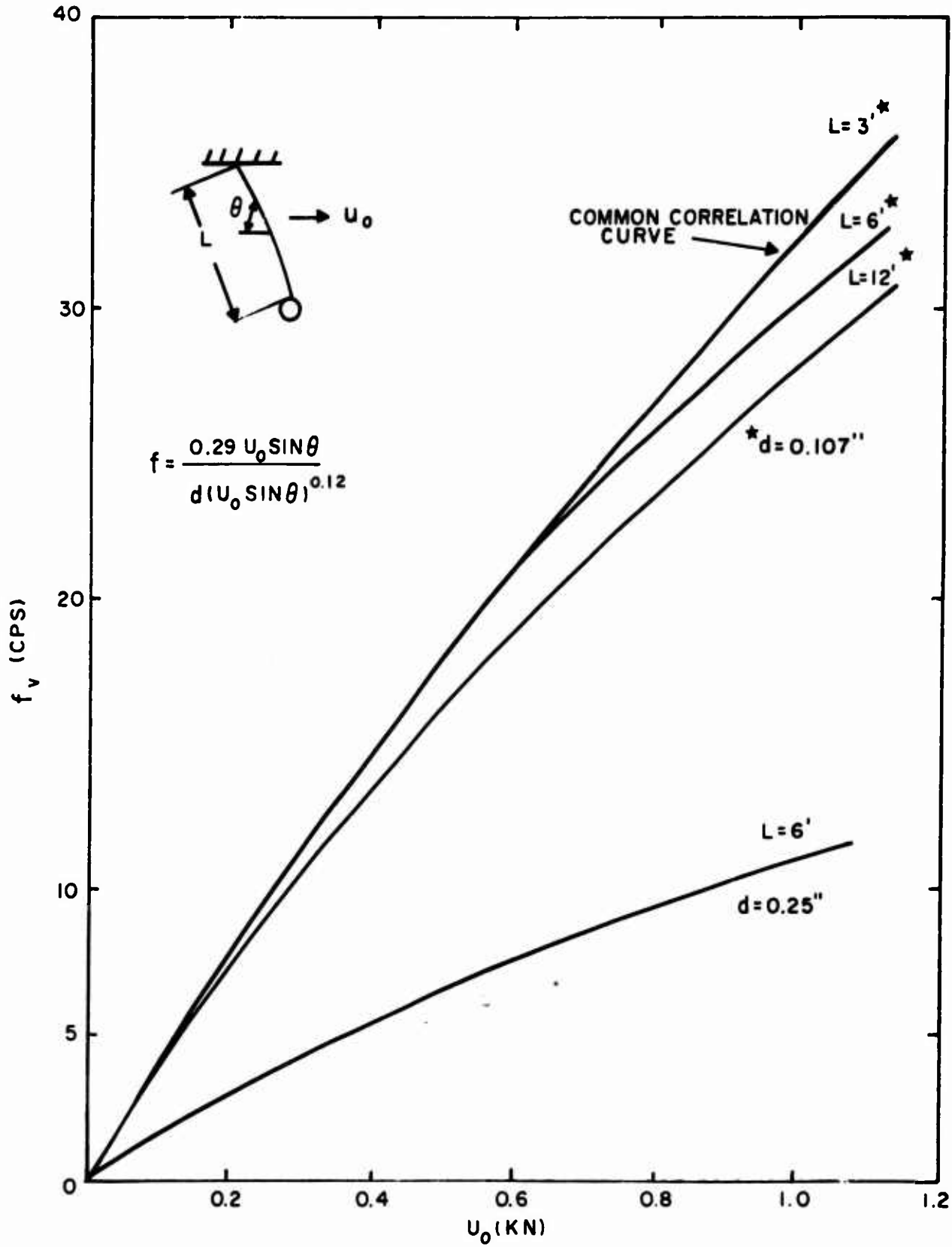0   0.2   0.4   0.6   0.8   1.0   1.2

U_0 (KN)

FIGURE 6 - Mean Frequency Plots for Various Cable Lengths and
Diameters with the Common Correlation Curve

These results are reasonable because a streaming cable with a terminal mass can be approximated by two tangent lines - one comparatively close to the mass and the other representing the major portion of the cable, of which the upper incidence angle is representative. This would imply that the upper portion of the cable is primarily responsible for the signal frequency at the terminal mass. The equation for this common correlation curve was obtained as,

$$f_V = \frac{0.29 \ u_o \ Sin \ \theta}{d \ (u_o \ Sin \ \theta)0.12}, \tag{4}$$

where u_o is in knots and d is in feet.

The velocity correction is assumed to be accounted for by the normal component $u_o \ Sin \ \theta$. Then the virtual diameter is,

$$d \ (u_o \ Sin \ \theta)0.12. \tag{5}$$

Thus, the virtual diameter increases as the free stream velocity increases or as the vibration frequency increases the cable appears to have a larger fluid dynamic diameter. Equation (4) predicted all the plots on figure 6 within ±5 percent.

MOTION OF TERMINAL MASS

A simplified analytical model of the fixed-end strumming cable support- ing a terminal mass was developed for correlation with the experimental results, and it is to be used as a basis for general scaling laws. The tractable model assumes that the suspension system can be represented by two intrinsic spring-mass system types. First, each standing wave represents a spring of length (ℓ) and a mass equivalent to the cable mass for the length (ℓ). An expression for the dynamic cable tension is then derived by assuming each standing wave system is in horizontal resonance with sinusoidal motion; second, the spring-mass system comprises the entire submerged cable length (L) as the spring and the terminal mass (W) as that which is forced harmonically by the dynamic cable tension in a direction parallel to the attached cable. The equation of motion is developed in appendix A and has the general form:

$$W\ddot{y} + r_m\dot{y} + \frac{K_y}{L} (\delta + y) - Wg = F(t). \tag{6}$$

When simplified, this results in the following expression for the acceler- ation of the terminal mass:

$$\ddot{y} = (\rho \ C_L)^2 \ \frac{d^2 \ K_y \ u_o^4}{rc^2 \sqrt{\left[\frac{K_y}{L} - W \ (2\omega_v)^2\right]^2 + r_m^2 \ \omega_v^2}} \ Cos \ (2\omega_v t - \alpha). \tag{7}$$

Two conclusions are apparent. First, since the frequency is $2\omega_v$, the signal frequency is twice the cable vibration frequency; second, the magnitude of $\ddot{y}$ will be sensitive to the cable spring constant (K_y). For any specific submerged cable length, there will be a value of ω_v or water velocity (u_o) at which the signal level will peak. (This critical condition has been defined as vertical resonance.) A review of the signal signatures for a decaying flow field does indeed reveal this predicted vertical resonance, even though the amplitude transitions tend to obscure the effect.

A series of runs were made for various cable lengths from 1 to 12 feet, and the signal amplitude variations were plotted using each standing wave length as the common parameter. This data is shown on figure 7 for standing wave lengths of 0.5, 1.0, 1.5, and 3.0 feet. The veritable resonant peaks are clearly shown for the shorter standing wave lengths, and they appear to shift to the longer cable lengths for the longer standing wave lengths. This shift is in agreement with the analysis, because as the cable length (L) increases the effective cable spring constant (K_y/L) decreases. Since this spring constant is largely responsible in predicting the resonant conditions, this implies that as K_y/L decreases, resonance will occur at lower frequencies which correspond to longer standing wave lengths.

The data points were taken at frequencies assumed to represent the true partial frequency for each standing wave - at the highest signal amplitude for that particular partial. Accordingly, the data points are sparse, particularly for the longer standing wave lengths, because data could only be obtained where the specific standing wave length represented an integral number of the cable length. Since the 12-inch standing wave was defined by more data points, this resonant peak was used to empirically determine the constant value of K_y (the spring constant per foot of cable). Using this value in the acceleration expression, equation (7), a plot equivalent to figure 7 was computed and is shown as figure 8. The physical system is clearly damped more than the analysis assumes, as shown by comparison of the resonant peaks. This can be accounted for because to linearize the differential equation damping was assumed to vary as the first power of velocity. Also, it is known that the relative cable velocity, which is the vector sum of the free stream and cable vibration velocities, is considerably larger than the assumed free stream velocity.

The shift in resonant peaks is clearly indicated by comparing figures 7 and 8. On figure 8, the portion of the curves to the right of resonance has a negative slope that tends to level off. The changing effective spring constant (K_y/L) has progressively less significance as compared to the w $(2\omega_v)^2$ term, where ω_v is fixed for a given value of L. This causes the curves to level off. The portions of the curves to the left of resonance have a sharper positive slope because K_y/L increases rapidly
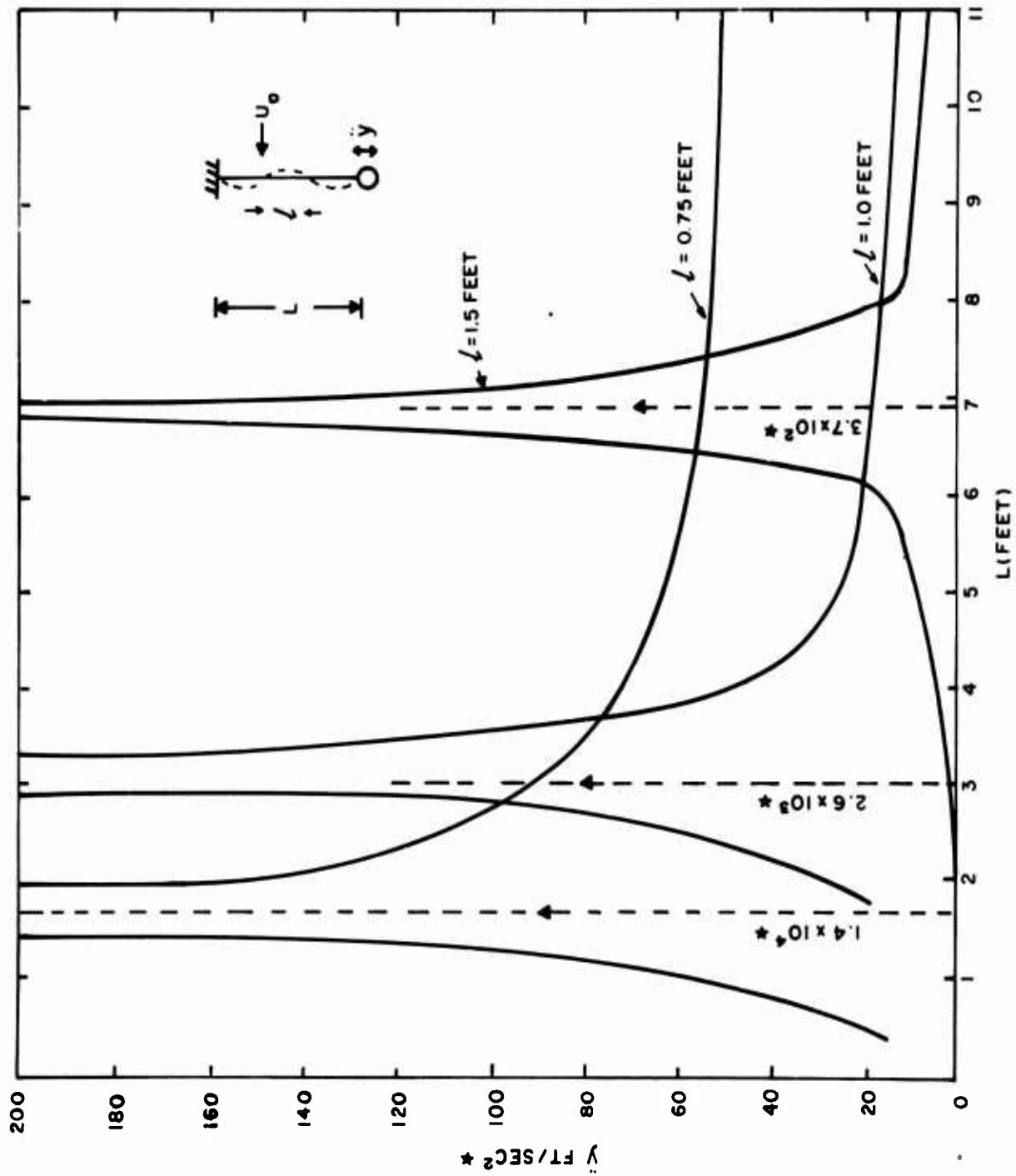
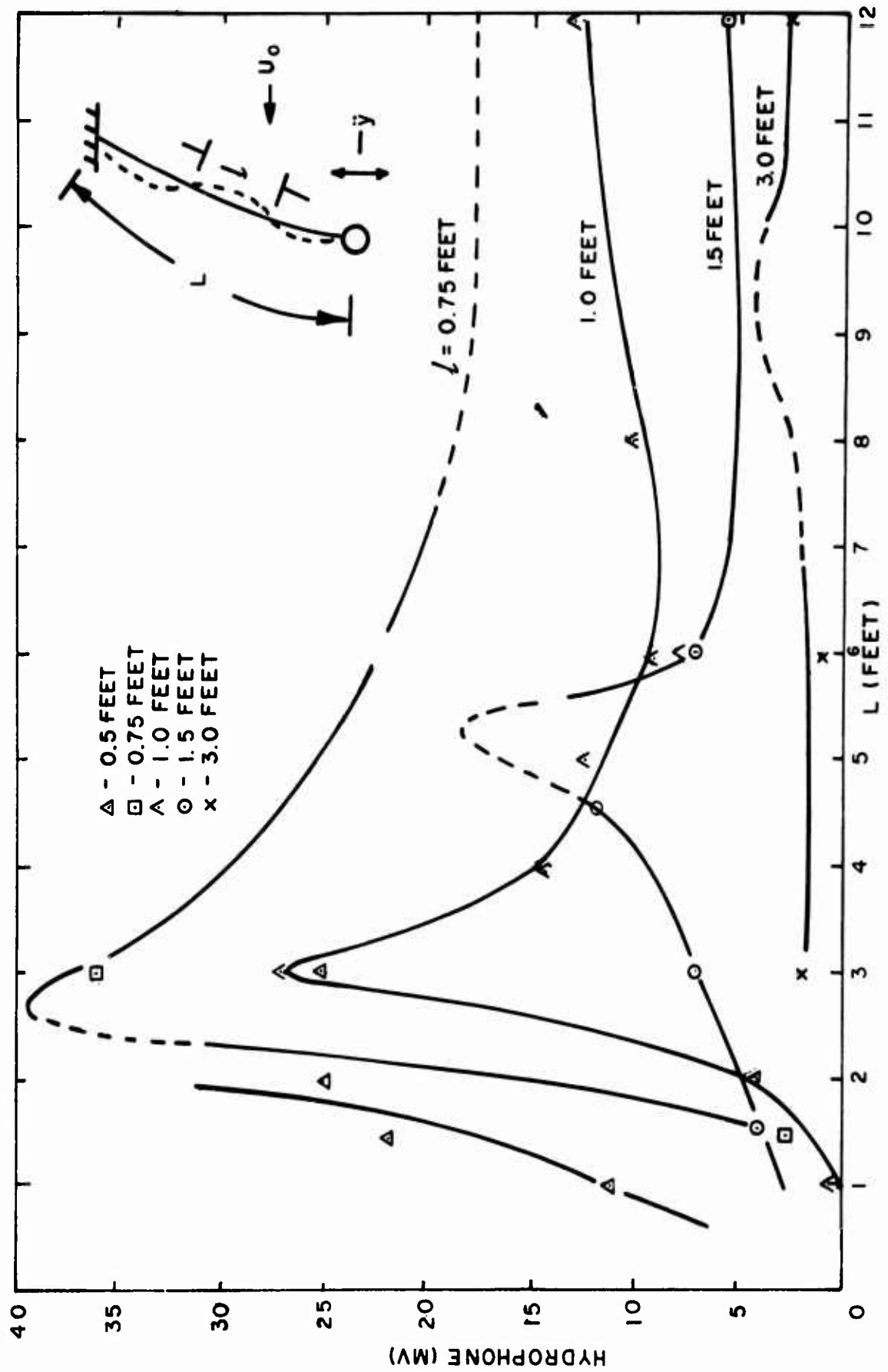FIGURE 7 - Experimental Motion Response of the Terminal Mass to Cable Strumming Forces

FIGURE 8 - Theoretical Acceleration Response of the Terminal Mass to Cable Strumming Forces

as compared to the constant value of the $W (2\omega_v)^2$ term. It should be noted that the sensitivity of the k_y/L term also appears to similarly control the respective slopes on the experimental plots, figure 7.

The correlation is indeed reasonable when consideration is given to the simplifying assumptions made in the equation derivation for linearization.

To demonstrate the effect of the shifting resonant peak, signal signatures were made for a 6-foot length of cable before and after a localized permanent kink was artificially placed in the cable. The cable was kinked to lower the effective spring constant. These records are shown in figure 9 and clearly indicate the resonant peak shift to a lower velocity. Both records were made through the same velocity range and by vertically aligning equivalent partial structures, the shift in amplitude is seen. For the strumming frequency range considered, a short compliant section is effective in reducing the magntiude of the mass acceleration and may prove useful for certain designs.

A portion of a partial vibration structure is also indicated on figure 9 wherein a marked peak can be observed at the high amplitude end of the structure. Observations indicate that this effect frequently shows up where the vertical resonant peak is at or near a water velocity corresponding to a true partial vibration. This effect is assumed to represent a coincidence of the vertical and horizontal resonance effects.
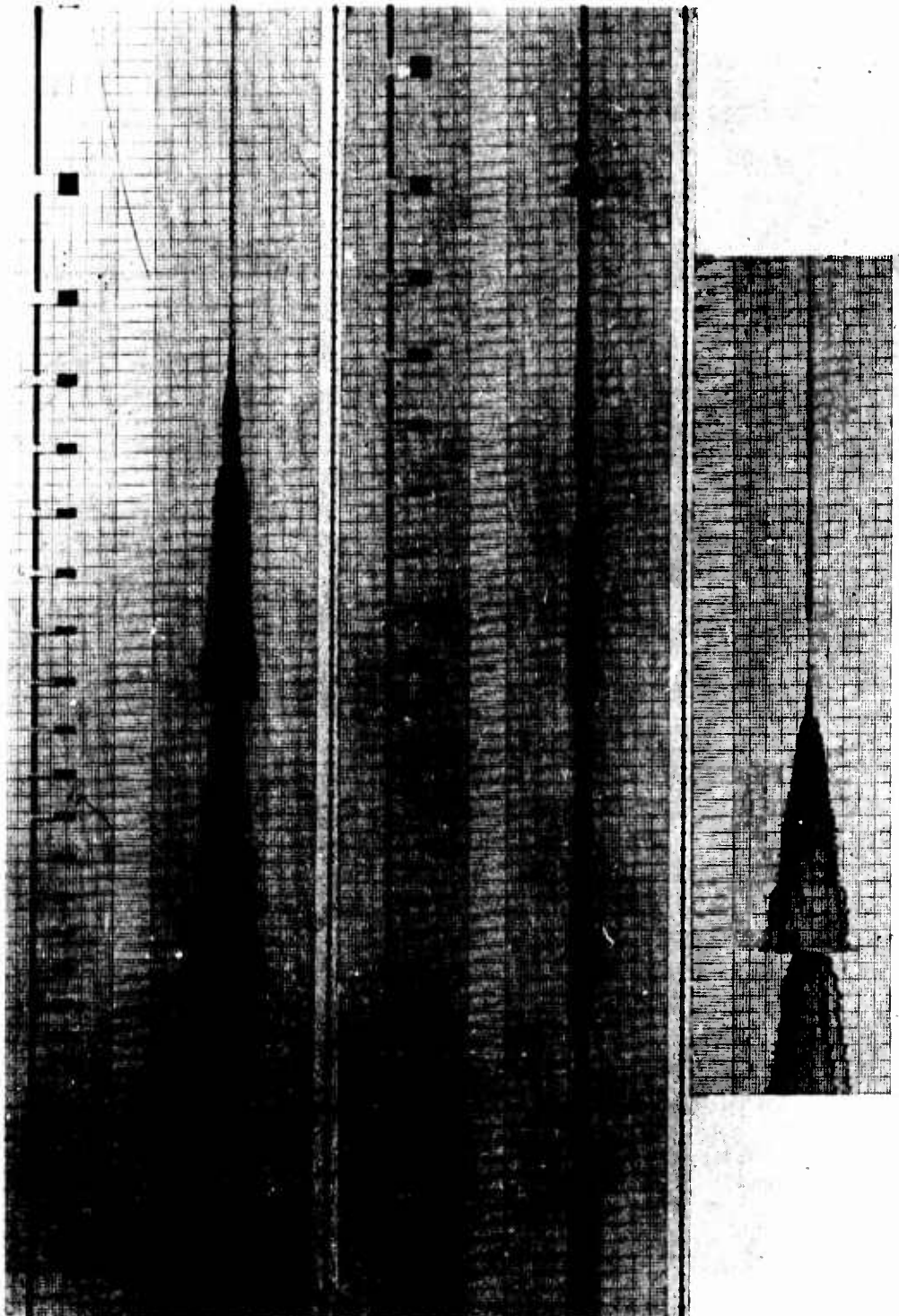
NOTE: THE TWO UPPER SIGNAL SIGNATURES SHOW THE RESONANCE PEAK SHIFT TO A LOWER VELOCITY AND THE OVERALL SIGNAL ATTENUATION AFTER KINKING A 6-FOOT CABLE. WATER VELOCITY DECREASES TO THE RIGHT FROM 1.2 TO 0.5 KNOTS INDICATED BY THE STEP PULSE INTERVAL FOR THE TOP AND CENTER RECORDS. TOP - BEFORE KINKING. CENTER - AFTER KINKING. THE BOTTOM RECORD SHOWS THE HIGH SIGNALS RESULTING WHEN HORIZONTAL AND VERTICAL RESONANCE OCCUR AT OR NEAR THE SAME FREQUENCY. 1 SECOND TIME PULSES ARE INDICATED BELOW EACH RECORD.

FIGURE 9 - Vertical Resonance Effects

A P P E N D I X   A

TERMINAL MASS MOTION ANALYSIS

- -

A rigorous motion analysis is not justified because of the lack of knowledge of the physical time variation of the various periodic fluid forces acting on a flexible cable. The derivation is simplified by appropriate assumptions to linearize the motion equations.

GENERAL ASSUMPTIONS

1. The cable-mass system hangs vertically, or static fluid drag forces are considered negligible.

2. Only the periodic fluid lift forces are considered, and they are assumed harmonic with time.

3. The dependent motion of the mass is vertical.

4. The cable is flexible and connotes the absence of any bending restoring forces.

5. Fluid damping of the cable and mass is proportional to the first power of velocity.

6. Steady-state motion of the terminal mass is analyzed where the mass follows the cable during the entire cycle. The mass is never in a free-fall state.

EQUATION OF MOTION

The cable-mass system is assumed to be represented schematically by a forced damped spring-mass analog, figure A-1. The periodic forcing function F(t) results from the fluid forced cable vibrations.
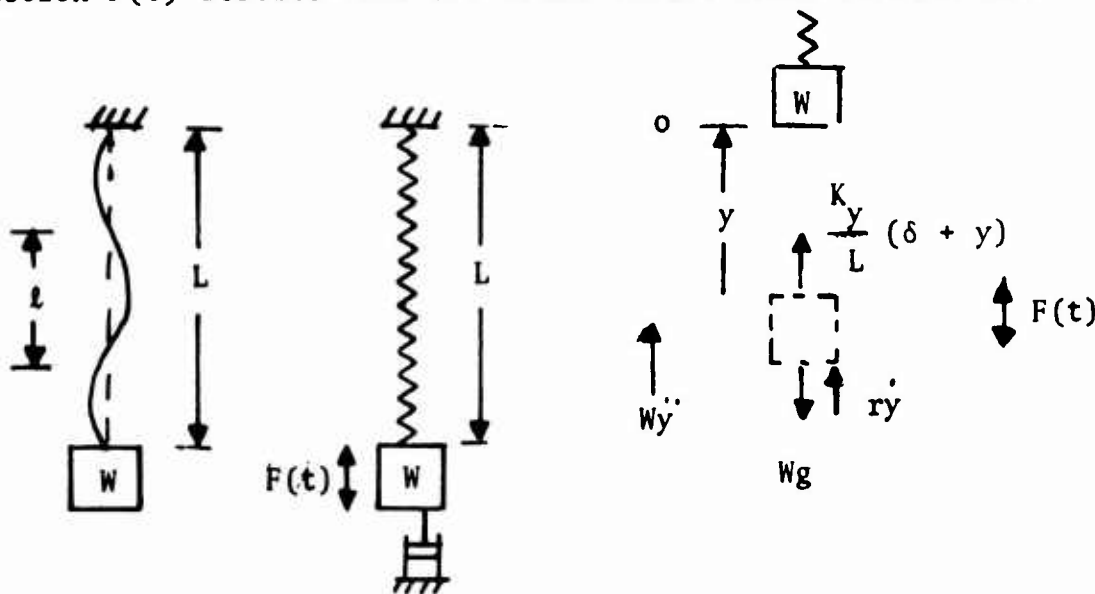
FIGURE A-1

The equation of motion can be written as the summation of all vertical forces:

$$W \ddot{y} + r_m \dot{y} + \frac{K_y}{L} (\delta + y) - Wg = F(t) \tag{A-1}$$

where K_y/L is the spring constant for a spring of length (L).

Since $(K_y/L)\delta = gW$, equation (A-1) reduces to

$$W \ddot{y} + r_m \dot{y} + \frac{K_y}{L} y = F(t). \tag{A-2}$$

FLUID FORCING FUNCTION

The derivation assumes that each standing wave of length (ℓ) can be represented by the spring mass system shown in figure A-2.
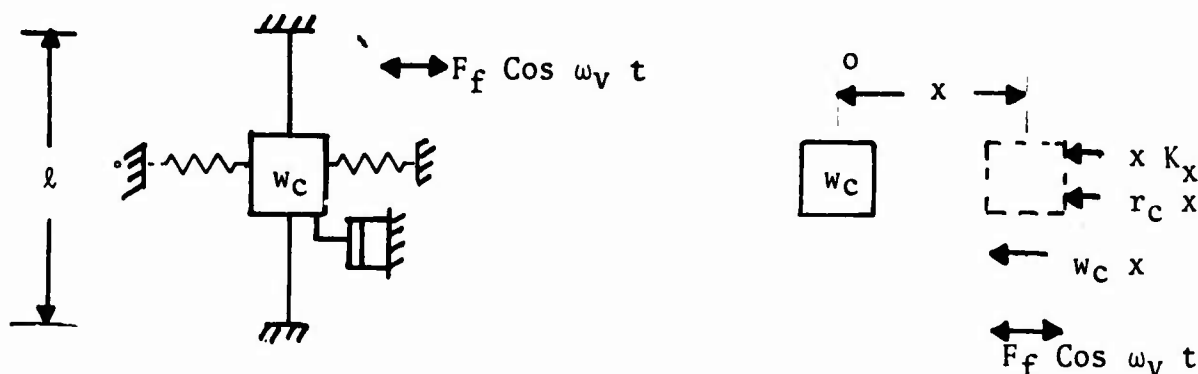
FIGURE A-2

The equation of motion is then a summation of the horizontal forces:

$$w_c \ddot{x} + r_c \dot{x} + K_x y = F_f \cos \omega_v t, \tag{A-3}$$

where F_f is the amplitude of the transverse periodic fluid lift force

$$F_f = \frac{C_L \, d \, \ell \, \rho \, u_o^2}{2}.$$

The particular integral of equation (A-3) is

$$x = \frac{F_f \; Cos \; (\omega_v \, t - \gamma)}{\sqrt{(K_x - w_c \, \omega_v{}^2)^2 + r_c \, \omega_v{}^2}}.$$

A true partial vibration is assumed for the standing wave of length (ℓ) or $w_c \, \omega_r{}^2 = k_x$ when $\gamma = 90$ degrees. Thus,

$$x = \frac{F_f \; Sin \; \omega_v \, t}{r_c \, \omega_v}. \qquad\qquad (A-4)$$

The periodic forcing function F(t) can be represented by the change in ℓ times the equivalent spring constant:

$$F(t) = \frac{K_y}{\ell} \, \Delta \, \ell$$

since

$$\Delta \, \ell = 2 \sqrt{x^2 + (\ell/2)^2} - \ell \simeq \frac{2x^2}{\ell};$$

therefore,

$$F(t) = K_y \left(\frac{2x^2}{\ell^2} \right)$$

Making use of the expression for X given by equation (A-4)

$$F(t) = \frac{2K_y}{\ell^2} \left[\frac{F_f \; Sin \; \omega_v t}{r_c \, \omega_v} \right]^2$$

or

$$F(t) = -\beta \; Sin^2 \; \omega_v t,$$

where

$$-\beta = 2K_y \left(\frac{F_f}{\ell \; r_c \; \omega_v} \right).$$

Since

$$\sin^2 \omega t = \frac{1 - \cos 2\omega t}{2},$$

$$F(t) = \frac{-\beta + \beta \cos 2\omega_V t}{2}. \tag{A-5}$$

Substitution in equation (A-2) gives

$$W\ddot{y} + r_m \dot{y} + K_y/L\, y + \beta/2 = \beta/2 \cos 2\omega_V t. \tag{A-6}$$

Let $a = W$, $b = r_m$, $C = K_y/L$, $e = \beta/2$, and $2\omega_V = h$.

For $t > 0$, the particular integral will be of the form:

$$y = -e/c + A \cos ht + \beta \sin ht$$

$$\dot{y} = \beta h \cos ht - A h \sin ht$$

$$\ddot{y} = -\beta h^2 \sin ht - A h^2 \cos h t.$$

Substitution into equation (A-6) and clearing the constants A and B yields,

$$y = -\frac{e}{c} + \frac{e\,[(c - ah^2)\cos ht + bh \sin ht]}{(c - ah^2)^2 + b^2 h^2}$$

Substituting the values for a, b, c, e, h, and β gives,

$$y = \frac{F_f^2}{\ell^2 r_c^2 \omega_V^2} \left\{ L - \frac{K_y}{\left[\dfrac{K_y}{L} - W(2\omega_V)^2\right]^2 + r_m^2 (2\omega_V)^2} \right.$$

$$\left. \left[\frac{K_y}{L} - W(2\omega_V)^2 \cos 2\omega_V t + r_m\, 2\omega_V \sin 2\omega_V t\right] \right\} \tag{A-7}$$

Adding the trigonometric functions within the brackets vectorally gives,

$$y = \frac{F_f^2}{\ell^2 \, r_c^2 \, \omega_v^2} \left\{ L - \frac{K_y}{\left[\frac{K_y}{L} - W \, (2\omega_v)^2 \right]^2 + r_m^2 \, (2\omega_v)^2} \right.$$

$$\left. \sqrt{\left[\frac{K_y}{L} - W \, (2\omega_v)^2 \right]^2 + (r_m \, 2\omega_v)^2} \; \cos(2\omega_v t - \phi) \right\} \qquad (A-8)$$

where

$$\phi = \text{Tan}^{-1} \frac{-2\omega_v r_m}{- \left[\frac{K_y}{L} - W \, (2\omega_v)^2 \right]}.$$

The corresponding expression for $\ddot{y}$ may be found by differentiation of equation (A-8):

$$\ddot{y} = \frac{4 \, K_y \, F_f^2}{\ell^2 \, r_c^2 \, \sqrt{\left[\frac{K_y}{L} - W \, (2\omega_v)^2 \right]^2 + r_m^2 \, (2\omega_v)^2}} \; \cos(2\omega_v t - \alpha) \qquad (A-9)$$

where

$$\alpha = \text{Tan}^{-1} \left[\frac{r_m \, (2\omega_v)}{\frac{K_y}{L} - W \, (2\omega_v)^2} \right],$$

since

$$F_f = \frac{C_L \, \ell d \, \rho \, u_o^2}{2},$$

Equations (A-8) and (A-9) can be rewritten in terms of all the known parameters of the system:

$$
y = \left(\frac{\rho \ C_L}{2}\right)^2 \frac{d^2 \ L \ u_o{}^4}{r_c{}^2 \ \omega_v{}^2} \left\{ 1 - \frac{K_y}{L\sqrt{\left[\dfrac{K_y}{L} - W \ (2\omega_v)^2\right]^2 + (2r_m\omega_v)^2}} \right\}
$$

$$
Cos \ (2\omega_v t - \phi) \tag{A-8a}
$$

$$
\ddot{y} = (\rho \ C_L)^2 \ \frac{d^2 \ K_y \ u_o{}^4}{r_c{}^2 \sqrt{\left[\dfrac{K_y}{L} - W \ (2\omega_v)^2\right]^2 + (2r_m \ \omega_v)^2}}
$$

$$
Cos \ (2\omega_v t - \alpha) \tag{A-9a}
$$

DOCUMENT CONTROL DATA - R&D

(Security classification of title, body of abstract and indexing annotation must be entered when the overall report is classified)

1. ORIGINATING ACTIVITY (Corporate author)	2a. REPORT SECURITY CLASSIFICATION
AERO-ELECTRONIC TECHNOLOGY DEPARTMENT U.S. NAVAL AIR DEVELOPMENT CENTER JOHNSVILLE, WARMINSTER, PENNSYLVANIA 18974	UNCLASSIFIED
	2b. GROUP

3. REPORT TITLE

DYNAMIC CHARACTERISTICS OF UNDERWATER CABLES FLOW INDUCED TRANSVERSE VIBRATIONS

4. DESCRIPTIVE NOTES *(Type of report and inclusive dates)*

5. AUTHOR(S) *(Last name, first name, initial)*

DALE, J., MENZEL, H., AND McCANDLESS, J

6. REPORT DATE	7a. TOTAL NO. OF PAGES	7b. NO. OF REFS
6 SEPTEMBER 1966	32	3 (FOOTNOTES)

8a. CONTRACT OR GRANT NO.	9a. ORIGINATOR'S REPORT NUMBER(S)
b. PROJECT NO. WEPTASK ASW213000/2011/W210-14-00 PROBLEM NO. 803	NADC-AE-6620
	9b. OTHER REPORT NO(S) (Any other numbers that may be assigned this report)
d.	

10. AVAILABILITY/LIMITATION NOTICES

DISTRIBUTION OF THIS DOCUMENT IS UNLIMITED.

11. SUPPLEMENTARY NOTES	12. SPONSORING MILITARY ACTIVITY
	NAVAL AIR SYSTEMS COMMAND DEPARTMENT OF THE NAVY

13. ABSTRACT

The dynamic behavior of strumming hydrophone cables associated with air-launched sonobuoy surveillance systems is reported for a 200 to 3000 Reynolds number range. The study techniques and the scaling laws have application wherever underwater flexible cables are employed. Results are reported in four specific areas: experimental diagnostic techniques, cable tuning effects, frequency scaling law, and dynamic motion analysis.

DD FORM 1 JAN 64 **1473**

14. KEY WORDS	LINK A		LINK B		LINK C	
	ROLE	WT	ROLE	WT	ROLE	WT
SONAR						
SURVEILLANCE SYSTEM						
HYDROPHONE CABLES						

INSTRUCTIONS